Dalton Transactions

PAPER

View Article Online
View Journal | View Issue

Cite this: *Dalton Trans.*, 2015, **44**, 12576

Zn^{II} and Hg^{II} binding to a designed peptide that accommodates different coordination geometries†

Dániel Szunyogh,[a] Béla Gyurcsik,[a,b] Flemming H. Larsen,[c] Monika Stachura,[d] Peter W. Thulstrup,[e] Lars Hemmingsen*[e] and Attila Jancsó*[a,b]

Received 9th March 2015,
Accepted 22nd May 2015

DOI: 10.1039/c5dt00945f

www.rsc.org/dalton

Designed metal ion binding peptides offer a variety of applications in both basic science as model systems of more complex metalloproteins, and in biotechnology, *e.g.* in bioremediation of toxic metal ions, biomining or as artificial enzymes. In this work a peptide (**HS**: Ac-SCHGDQGSDCSI-NH_2) has been specifically designed for binding of both Zn^{II} and Hg^{II}, *i.e.* metal ions with different preferences in terms of coordination number, coordination geometry, and to some extent ligand composition. It is demonstrated that **HS** accommodates both metal ions, and the first coordination sphere, metal ion exchange between peptides, and speciation are characterized as a function of pH using UV-absorption-, synchrotron radiation CD-, ^{1}H-NMR-, and PAC-spectroscopy as well as potentiometry. Hg^{II} binds to the peptide with very high affinity in a {HgS_2} coordination geometry, bringing together the two cysteinates close to each end of the peptide in a loop structure. Despite the high affinity, Hg^{II} is kinetically labile, exchanging between peptides on the subsecond timescale, as indicated by line broadening in ^{1}H-NMR. The Zn^{II}-**HS** system displays more complex speciation, involving monomeric species with coordinating cysteinates, histidine, and a solvent water molecule, as well as **HS**-Zn^{II}-**HS** complexes. In summary, the **HS** peptide displays conformational flexibility, contains many typical metal ion binding groups, and is able to accommodate metal ions with different structural and ligand preferences with high affinity. As such, the **HS** peptide may be a scaffold offering binding of a variety of metal ions, and potentially serve for metal ion sequestration in biotechnological applications.

Introduction

Metal sensor proteins[1–5] display high selectivity for both essential and toxic metal ions, as demonstrated by representative members of the MerR family,[6,7] such as the Cu^{I}-sensing CueR, Zn^{II}-sensing ZntR, and Hg^{II}-sensing MerR.[8] In this work we have attempted to design a peptide with a broader metal ion binding profile. In a biotechnological perspective, overexpression of such a peptide in suitable bacteria could endow the cells with the capacity to sequester metal ions, including toxic elements, from the environment.[9] Additionally, elevated levels of such a peptide could ensure metal ion buffering of the cytosol, allowing the bacterium to survive in harsh conditions of both deprivation and over-exposure to metal ions in the surrounding medium, and serve as an engineered organism with improved properties for biomining and bioremediation.[10–12] The template for the design was the Cu^{I} binding loop of CueR from *V. cholerae*, SCPGDQGSDCP. In the related sequence from *E. coli*, Cu(I) ion is coordinated by two cysteines in a linear coordination geometry.[8] The peptide is also expected to possess the capacity to bind the soft Hg^{II} ion, due to the thiophilicity of this ion. In order to broaden the metal ion binding profile, and increase the peptide solubility, proline to histidine and proline to serine substitutions were introduced at positions 3 and 11, respectively. The positions of substitutions were chosen to increase ligand-flexibility, and to mimic the presence of His and Ser at these positions in some of the metalloregulatory MerR family members.[8] The modifications were expected to promote the coordination of the borderline soft/hard Zn^{II} ion. In a recent study we demonstrated that this designed 12-mer **HS** peptide (see Scheme 1) forms various species with Cd^{II}, including loop structures and metal ion bridged bis-ligand complexes, depending on pH and metal to ligand ratio.[13]

Zn^{II} is rather promiscuous in terms of coordination characteristics as compared to the clearly soft, often two-coordinated

[a]*MTA-SZTE Bioinorganic Chemistry Research Group, Dóm tér 7, Szeged, H-6720, Hungary*
[b]*Department of Inorganic and Analytical Chemistry, University of Szeged, Dóm tér 7, Szeged, H-6720, Hungary. E-mail: jancso@chem.u-szeged.hu; Fax: (+36) 62544340*
[c]*Department of Food Science, University of Copenhagen, Rolighedsvej 30, 1958 Frederiksberg C, Denmark*
[d]*CERN, 23 Geneva, 1211-Geneva, Switzerland*
[e]*Department of Chemistry, University of Copenhagen, Universitetsparken 5., 2100 Copenhagen, Denmark. E-mail: lhe@chem.ku.dk; Fax: (+45) 35332398*
†Electronic supplementary information (ESI) available. See DOI: 10.1039/c5dt00945f

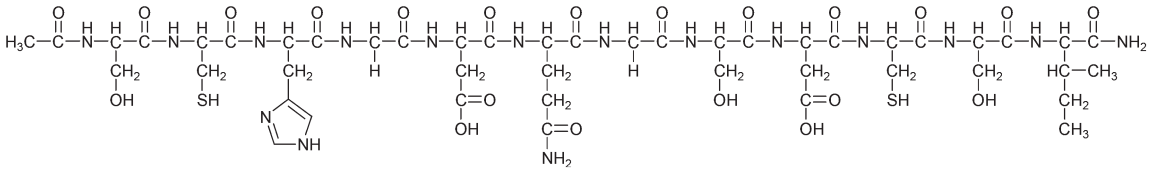

Scheme 1 Schematic structure of Ac-SCHGDQGSDCSI-NH_2 (**HS**).

Hg^{II}. In general, Zn^{II} can easily adopt four-, five- or six-coordinate environments.[14] Nevertheless, in zinc-containing enzymes and proteins the most typical coordination number is four.[14,15] The preference of Zn^{II} for a tetrahedral coordination geometry in proteins is supported by detailed statistical analyses of crystal structures of zinc-containing proteins deposited in the Protein Data Bank (PDB).[16,17] Five- and six-coordinated Zn^{II} centers are typically present due to the complementary coordination of solvent or inhibitor molecules in zinc-containing enzymes.[17] Depending on the type of zinc-centers the abundance of Cys and His side chains significantly varies in the donor set patterns (number and type of bound donor groups). At catalytic zinc-centers any three N, O or S donors of Cys, His, Asp and Glu residues bind Zn^{II} in a 4–5 coordinate distorted-tetrahedral or trigonal-bipyramidal geometry, with His being the predominant ligand.[18] A water molecule is always found in such centres. His and Asp donors are dominant at the co-catalytic zinc-sites consisting of two or three metal ions in close proximity, two of which are bridged by one of the amino acid side chains or a water molecule.[18] Cysteines, however, are not utilized at these motifs. Four protein side chain ligands are bound to Zn^{II} in a tetrahedral or distorted tetrahedral geometry at structural zinc-sites.[18] Such a binding mode is characteristic for *e.g.* the nucleic acid binding zinc finger proteins[15] and for the zinc-clusters in metallothioneins.[19] In all classes of the structurally diverse zinc fingers[20,21] Zn^{II} ions are ligated by a combination of four Cys/His side chain donors, at least two of which are Cys thiolates.[15] Thiolate donors, complemented with side chain carboxylates and His-imidazoles, are also typical at the metalloregulatory Zn^{II} binding sites in various zinc sensor proteins, however, coordination number and geometry appears to be more decisive in metal ion selectivity than donor ligand types.[15]

Hg^{II} can tolerate various coordination numbers and geometries, although, six-coordination is much less common than for the other two group 12 metal ions Cd^{II} and Zn^{II}.[22] Linear two-coordinate, trigonal planar or T-shaped three-coordinate or tetrahedral four-coordinate structures are representative for complexes with monodentate ligands and higher coordination numbers might be accessible mostly with multidentate compounds.[22,23] Hg^{II} forms complexes with coordination number 2 more commonly than any other metal ion,[22] which can be explained by relativistic effects.[24] Low coordination numbers are characteristic for complexes formed with thiolates, a class of ligands displaying an outstanding affinity towards the large and soft Hg^{II} ion,[25] and in biological systems Hg^{II} is usually complexed by low molecular weight thiolates or by the Cys side chains of proteins.[26] Amongst others, some representative examples are provided by the bacterial mercury resistance systems, *e.g.* MerP where Hg^{II} is bound to a CXXC (X = amino acid other than cysteine) fragment in a typical linear two-coordinate fashion,[27] or the metalloregulatory protein MerR where Cys residues from the two protein monomers form a tri-coordinate metal binding site for Hg^{II}.[28,29] Additionally, distorted tetrahedral Hg^{II} coordination environment was reported in a few Hg^{II}-substituted proteins.[30–32]

The substantially different preferences of Zn^{II} and Hg^{II} for four- and two-coordinated structures and the negligible role of His side chains in Hg^{II} biocoordination prompted us to investigate whether the His residue incorporated in the flexible ligand sequence of **HS** might have an influence on the binding of either of the two metal ions. In this work we characterize the binding of Zn^{II} and Hg^{II} to the peptide in terms of the metal site coordination geometry and exchange dynamics.

Results and discussion

UV absorption and SRCD studies monitoring the formation of thiolate–metal ion bonds and ligand structure

Comparison of pH-dependent series of UV-spectra in the presence of 0, 0.5 and 1.0 equivalent of Hg^{II} or Zn^{II} as compared to the ligand provides information on the interaction of the metal ions with donor groups of **HS**. The occurrence of $S^- \rightarrow Hg^{II}$ ligand to metal charge transfer (LMCT) transitions[25,33–35] upon the addition Hg^{II} to the peptide imply that the cysteine side chain thiolate groups of the ligand are coordinated to Hg^{II} already at low pH (see the full spectra in ESI, Fig. S1A–B†). The Hg^{II} : **HS** 1 : 1 system shows almost a constant absorbance at λ = 230 nm at pH = 4–11 that is significantly higher than the absorption observed for the ligand in the absence of metal ion between pH ~ 4.0–9.0 (Fig. 1). This suggests that the thiolate groups of **HS** are bound to Hg^{II} from acidic to alkaline pH. It is important to note that the deprotonation of the cysteine residues of the free peptide between pH ~ 8–10 is accompanied by the appearance of an $n \rightarrow \sigma^*$ transition around 230–240 nm characteristic for deprotonated thiols[36,37] (Fig. 1 and S2†), and as this is absent for the Hg^{II}-**HS** species, we infer that the $\{HgS_2\}$ coordination geometry is formed at pH lower than 4.

The pH-dependent absorbances detected for the sample containing 0.5 equivalent of Hg^{II} compared to **HS** are in between the values observed for the ligand alone and the

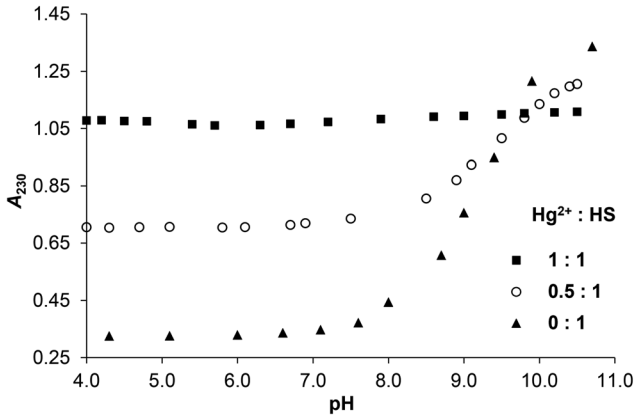

Fig. 1 Change of the measured absorbances at 230 nm as a function of pH in the Hg^{II} : **HS** 1 : 1, 0.5 : 1 and 0 : 1 systems (c_{HS} = 1.0 × 10^{-4} M, I = 0.1 M $NaClO_4$, T = 298 K).

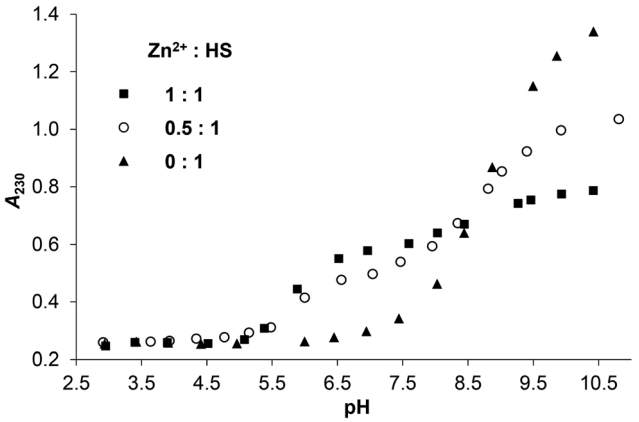

Fig. 2 Change of the measured absorbances at 230 nm as a function of pH in the Zn^{II} : **HS** 1 : 1, 0.5 : 1 and 0 : 1 systems (c_{HS} = 1.0 × 10^{-4} M, I = 0.1 M $NaClO_4$, T = 298 K).

Hg^{II}–**HS** 1 : 1 system at any pH (Fig. 1). This suggests that ~50% of the cysteine residues are bound to Hg^{II} even under acidic conditions and the remaining thiol groups deprotonate in parallel with the free ligand. The spectra recorded in the presence and absence of Hg^{II} reflect that the $S^- \rightarrow Hg^{II}$ charge transfer transitions are located below λ = 220 nm ($\varepsilon_{215\ nm}$ ~ 15 900 M^{-1} cm^{-1}) independently of the pH and metal ion to ligand ratio (see the difference spectra of Hg^{II}–**HS** 1 : 1 and the free ligand in Fig. S3†). Such high energy LMCT transitions and the observed molar absorbances imply that two thiolates are coordinated to the metal ion, as proposed in previous reports on Hg^{II} – oligopeptide model systems.[38–42] Three or four Hg^{II}-bound thiolates in a trigonal/tetrahedral coordination geometry would result in LMCT peaks or shoulders at lower energies[25,31,35,40,42–44] which is not observed here even in the excess of **HS** over Hg^{II} indicating that metal ion bridged species are not formed.

In contrast to Hg^{II}, the LMCT band characteristic for S^-–Zn^{II} interactions in zinc(II)-bound proteins[32–34] and peptides[45–49] emerges only above pH ~ 5.0 in the solutions of Zn^{II} and **HS** (Fig. 2 and S4A–B†), reflecting the expected, substantially weaker affinity of Zn^{II} towards the ligand. A remarkable spectral change, *i.e.* a further absorbance increase occurs above pH ~ 7.5 in the presence of one equivalent Zn^{II} per **HS**. A similar, but less pronounced spectral change, attributed to the formation of hydroxo mixed ligand species, was also observed in the Zn^{II}-complex of a related 12-mer peptide,[50] however, at a higher pH. Thus, the metal bound water appears to display a lower pK_a of 8.65 in the Zn^{II}-**HS** complex, *vide infra* (potentiometric data).

The $A_{230\ nm}$ *vs.* pH curve obtained for the Zn^{II}–**HS** 0.5 : 1 sample runs in between those of the free peptide and the equimolar system in the whole studied pH-range (Fig. 2). The observed profile is closer to that seen in the presence of 1 eq. Zn^{II} between pH 5–9, contrary to the data recorded for Hg^{II}. Thus, a more complex speciation must occur for Zn^{II}, with more than half of the thiolates bound to the metal ion at a stoichiometry of 0.5 : 1 Zn^{II} : **HS**, indicating the formation of metal bridged species. At high pH, however, the absorbances detected for twofold ligand excess seem to be *ca.* the averages of those of the free ligand and the equimolar sample (see Fig. 2, S2 and S4†), suggesting similar speciation at any metal ion to ligand ratios.

In order to gain information on the metal ion induced conformational change of the peptide SRCD (synchrotron radiation circular dichroism) spectra were recorded both for Hg^{II} and Zn^{II} complexes. Previously we have demonstrated that **HS** displays a disordered structure with varying levels of transient helicities,[13] represented by an intense negative CD-extremum slightly below 200 nm and a less intensive shoulder around 220 nm.[34,47,51,52] Addition of Hg^{II} to the acidic solution of **HS** results in a notable decrease of the negative peak at λ ~ 198 nm while the shoulder is less affected (Fig. 3). A similar type of change was reported to accompany the Hg^{II}-coordi-

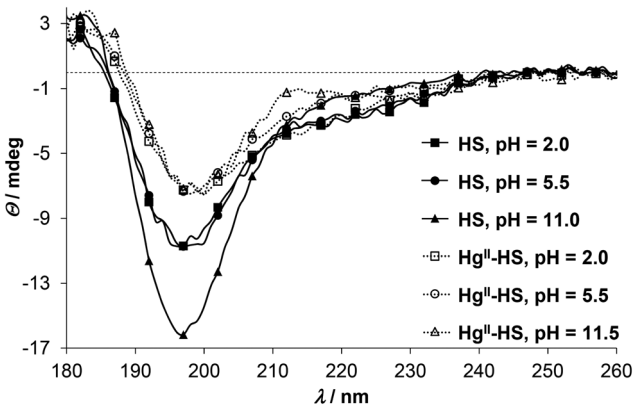

Fig. 3 SRCD spectra of HS in the absence (continuous lines with filled markers) and presence of 1.0 eq. of Hg^{II} (dotted lines with open markers) at selected pH values (c_{HS} = 1.0 × 10^{-3} M, I = 0.1 M $NaClO_4$, T = 298 K, l = 0.1 mm).

nation of a 18-mer peptide, comprising the metal binding loop of MerP possessing a CAAC motif.[53,54] The spectral change was assigned to the folding of the peptide to a thermodynamically (but not necessarily kinetically) stable conformation,[53] although the reduction of the negative ellipticity around 200 nm was also observed with other metal ions and two other peptide derivatives with alterations in the metal binding sequence (CCAA and CACA).[54] By all accounts, Hg^{II}-binding to **HS** clearly induces a conformational change of the ligand towards a loop structure, presumably similar to the metal-loaded forms of CueR.[8] One, however, has to bear in mind that due to the high energy ligand to metal charge transfer bands of the Hg^{II}-bound species, CD features of these bands may overlap with the backbone-related CD-effects. This is a known problem in the interpretation of the secondary structures of metalloproteins and metal ion–peptide complexes,[34,45,55,56] particularly when relatively small molecules, like the present 12-mer **HS** peptide, are studied. Distinction of the different contributions may be easier when thiolate to metal ion transitions appear separately at lower energies compared to the peptide backbone bands, like in the tetrahedral $\{CysS_4\}$ type Hg^{II}-rubredoxin complex[31] or in metallothioneins, where metal induced bands dominate the wavelength region above 220–230 nm.[57] Comparison of the SRCD spectra of **HS** at pH ~ 2.0 in the presence and absence of Hg^{II} (Fig. 3) suggests that any effect of the Hg^{II}-binding of the thiolate donors dominate below $\lambda \sim 210$ nm. The increase of pH has practically no further effect on the ellipticity around 198 nm for the Hg^{II}-**HS** complex, however, it slightly influences the lower energy shoulders. This can be assigned to the deprotonation of the Asp and His residues of the peptide inducing modest changes in the backbone of the loop-forming ligand.

Zn^{II} has no impact on the SRCD spectra of **HS** up to pH 5.5 (Fig. 4), which correlates well with the UV-spectra where the LMCT bands emerge above pH ~ 5. At higher pH, however, the position of the main negative CD-minimum is slightly red-shifted (see spectra at pH = 7.5 and 10.5 on Fig. 4), while the ellipticities around 180 and 230 nm are remarkably increased, as compared to the spectra of the free ligand. As hinted already for Hg^{II}, influences of the S^{-}–Zn^{2+} chromophore and the peptide secondary structure may be superposed in the observed CD-pattern of Zn^{II}-protein/peptide structures.[34,55,56] Nevertheless, the direction of the observed changes is rather similar to the Zn^{II}-induced effects on the conformation of a phytochelatin analogue[47] and other relatively short oligo-peptides[52,58] and may suggest an increasing helical content[47,52] in the Zn^{II}-bound **HS**. It was proposed that different coordination properties of metal ions may develop selectivity in the stabilization of the α-helical conformation of 20-mer peptides.[58] The fundamentally distinct CD-features of **HS** in the presence of Hg^{II} and Zn^{II} may imply that the different coordination geometry preference of the two metal ions promote large dissimilarity between the Hg^{II}- and Zn^{II}-bound structures of the ligand. The characteristic shoulder seen in the spectra of Zn^{II}-**HS** (Fig. 4 and S5†) starts to develop from *ca.* pH 6 (data not shown) but increases up to pH 9.5–10. The Zn^{II} : **HS** ratio dependence of the discussed CD-peak at pH 10.5 reflects a simple equilibrium between the free and Zn^{II}-bound **HS** (Fig. S5†).

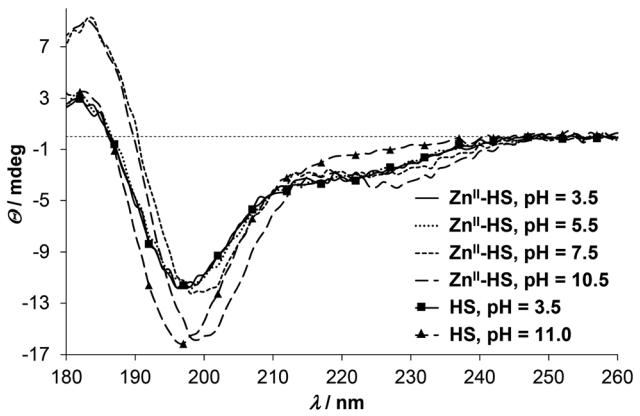

Fig. 4 pH-Dependent SRCD spectra recorded in the Zn^{II}–HS 1 : 1 system. pH = 3.5: continuous line; pH = 5.5: dotted line; pH = 7.5: short dashes; pH = 10.5: long dashes. For comparison, spectra of the free ligand is also shown at pH = 3.5 (continuous line with squares) and 11.0 (long dashes with triangles) (c_{HS} = 1.0 × 10^{-3} M, I = 0.1 M $NaClO_4$, T = 298 K, l = 0.1 mm).

^{199m}Hg PAC spectroscopy for the elucidation of the coordination environment of Hg^{II}

The local environment and coordination geometry of Hg^{II} was also monitored by ^{199m}Hg PAC (perturbed angular correlation of γ-rays) spectroscopy in the presence of one equivalent metal ion at pH = 2.0 and pH = 8.0. The fundamentals of PAC spectroscopy and the interpretation of the parameters obtained by the technique are described in detail in the literature.[59] The PAC data may be analyzed with one nuclear quadrupole interaction (NQI) at each pH, and the PAC parameters (ν_Q, the nuclear quadrupole coupling constant, and η, the so called asymmetry parameter, which is zero for an axially symmetric coordination geometry) for the observed NQIs are collected in Table 1. The fitted ν_Q and η values are similar at pH 2.0 and 8.0 and comparable to literature data obtained for compounds with two-coordinate $\{HgS_2\}$ structures[60,61] (Table 1). The spectrum recorded at low pH is slightly more complex than that obtained at pH ~ 8.0 as reflected in the lower signal amplitude and the broader and less visible second and third peaks, respectively (Fig. 5). This may suggest the co-existence of a small amount of species with a different structure, nevertheless, the main spectral features, with a support of UV-data, clearly indicate that the major component has a two-coordinate $\{HgS_2\}$ coordination mode.

Potentiometric investigation of distribution and stabilities of the species formed in the Zn^{II} : HS system

The formation constants ($\log \beta$) determined for the proton and Zn^{II} complexes of **HS** are summarized in Table 2.

The ligand undergoes five (de)protonation processes in the studied pH-range that were attributed to the carboxylate

Table 1 PAC parameters fitted for Hg^{II} : **HS** and for different Hg^{II}–thiolate complexes of known structures

System/pH	ν_Q/GHz	η	Coordination geometry	Ref.
Hg^{II}-**HS** 1 : 1 (pH = 2.0)	1.43(5)	0.07(6)	Two-coordinate, 2 thiolates	This work
Hg^{II}-**HS** 1 : 1 (pH = 8.0)	1.43(1)	0.13(3)	Two-coordinate, 2 thiolates	This work
$[Hg(Cysteine)_2]$	1.41	0.15	Two-coordinate, 2 thiolates	60
Ac-Cys-dPro-Pro-Cys-NH_2	1.42	0.19	Two-coordinate, 2 thiolates	41
MerA (77 K)	1.42	0.15	Two-coordinate, 2 thiolates	61
MerR (77 K)	1.18	0.25	Three-coordinate, 3 thiolates	61
Hg-rubredoxin	0.10	0 (fixed)	Four-coordinate, 4 thiolates	31

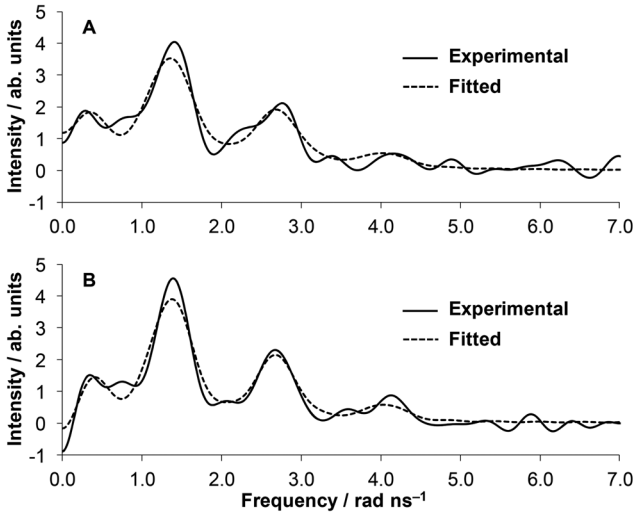

Fig. 5 Fourier transformed experimental (solid lines) and fitted (dashed lines) ^{199m}Hg PAC data of the Hg^{II} : **HS** 1 : 1 system at pH = 2.0 (A) and pH = 8.0 (B) ($c_{Hg^{II}} = c_{HS} = 8.03 \times 10^{-5}$ M).

groups of two Asp residues (pH ~ 3–5), the imidazole side chain of His (pH ~ 6–7.2) and the thiol moieties of the two Cys units (pH ~ 7.8–9.7).[13] The deprotonation constants (pK_a) of the ligand have been re-determined for the present study and are in a good agreement with those published earlier.[13]

In Table 2 the species model obtained by best fit of the Zn^{II} : **HS** system titration curves is presented. Introducing bis-ligand complexes (ZnH_xL_2) in the model was necessary for the correct description of titration data when **HS** was used in excess over Zn^{II} (see Experimental). Contrary to this, considering the presence of dinuclear species (Zn_2H_xL), did not improve the fit of the experimental data neither for the Zn^{II} : **HS** 0.5 : 1 and 1 : 1 samples nor for those containing a two-fold Zn^{II}-excess over the ligand (the latter was evaluated only up to pH ~ 7).

Table 2 Formation constants ($\log\beta$) of the Zn^{II} complexes of **HS** (estimated errors in parentheses (last digit)) and derived equilibrium data (I = 0.1 M $NaClO_4$, T = 298 K)

Species[a]	pqr[b]	$\log\beta_{pqr}$		pK_{pqr}[c], $\log K_2$[d]
$[ZnHL]^-$	111	16.58(4)	pK_{111}	5.95
$[ZnL]^{2-}$	101	10.63(4)	pK_{101}	8.65
$[ZnH_{-1}L]^{3-}$[e]	1–11	1.98(5)		
$[ZnH_2L_2]^{4-}$	122	31.3(2)	pK_{122}	7.6
$[ZnHL_2]^{5-}$	112	23.7(1)	pK_{112}	8.7
$[ZnL_2]^{6-}$	102	15.0(2)		
NP[f]		544	$\log K_2^L$	4.37
FP[g](cm^3)		0.005		

[a] $\log\beta$ values for the protonation processes of **HS**, re-determined in the present study are: $\log\beta_{051}$ = 31.68, $\log\beta_{041}$ = 28.33, $\log\beta_{031}$ = 24.10, $\log\beta_{021}$ = 17.50, $\log\beta_{011}$ = 9.06. [b] p,q, and r reflect stoichiometric numbers of the fundamental components the complex species are composed of, as defined in the experimental section. [c] $pK_{pqr} = \log\beta_{pqr} - \log\beta_{p(q-1)r}$. [d] $\log K_2 = \log\beta_{102} - \log\beta_{101}$. [e] H_{-1} represents an extra deprotonation, beyond the proton releases of the peptide, *i.e.* deprotonation of a Zn^{II}-bound water molecule. [f] NP = number of points. [g] FP = fitting parameter representing an average deviation in cm^3 between the experimental and fitted data for the full data set (including all evaluated titrations).

Complex formation processes start from pH ~ 4.5 by the appearance of a protonated mono-complex ZnHL as reflected by the calculated species distributions (Fig. 6). A consecutive deprotonation process ZnHL → ZnL + H^+ leads to the formation of the parent complex ZnL where all of the dissociable protons of the peptide are already released. The pK_a value for this process (= 5.95, see Table 2) is significantly lower than those attributed to the deprotonation processes of the HL and H_2L forms of the free ligand (pK_{HL} = 9.06, pK_{H_2L} = 8.44) and somewhat below the third pK_a of **HS** (pK_{H_3L} = 6.60). This strongly suggests that at least two, but potentially all the three neutral/basic donor groups of the ligand (histidine imidazole and two cysteine thiolates) are bound to Zn^{II} in the ZnL species. Coordination of both cysteines to Zn^{II} in ZnL is also supported by the observed absorbance increase in parallel with the formation of ZnHL/ZnL (A_{230} traces are overlaid with species distributions calculated for the concentration of UV data, see Fig. S6A–B†).

The determined stability of ZnL ($\log K$ = 10.63) reflects a remarkable affinity of **HS** to Zn^{II}. This stability constant is, indeed, several orders of magnitude higher than those of the parent Zn^{II} complexes of shorter peptides containing a CXH motif,[62] but also surpasses the stabilities of terminally protected tripeptides composed of a CXC sequence,[62] in spite of the substantially longer peptide chain and the larger distance between the two Cys residues in **HS**. Besides, **HS** has a notably higher affinity to Zn^{II} compared to a similar 12-mer oligopeptide possessing no histidine residues (studied by us, $\log K$ = 9.93).[50] Although higher stabilities were found for the Zn^{II} complexes of some 10-mer peptides, all of these contained 2–3 histidines in addition to the two cysteine units.[63] Thus, the affinity of **HS** for Zn^{II} falls in range that indicates the coordination of both cysteine and the histidine residues to the

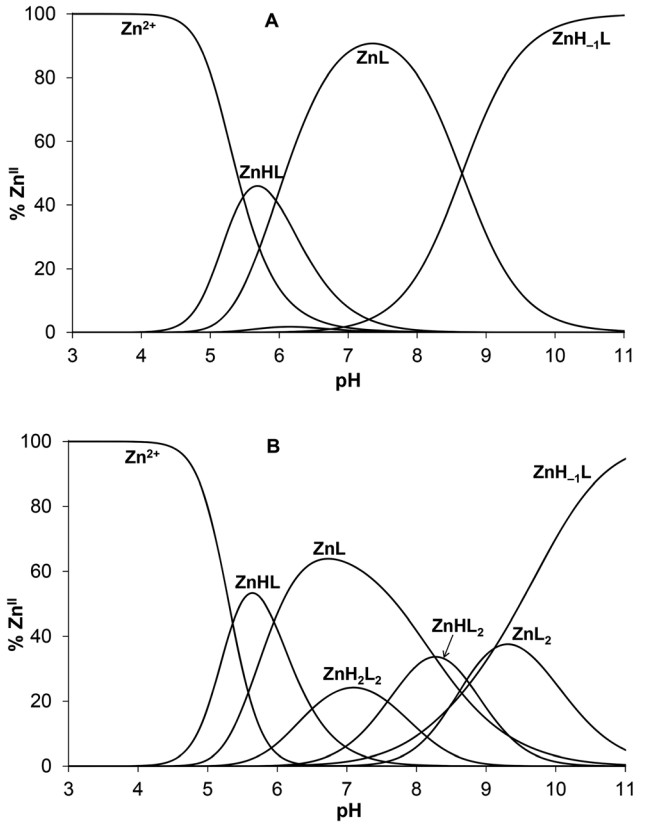

Fig. 6 Species distribution diagram for the Zn^{II} : HS 1 : 1 (A) and 0.5 : 1 (B) systems (c_{HS} = 1.0 × 10^{-3} M). The speciation curves for the concentrations applied in the UV experiments are depicted in ESI (Fig. S6A–B†).

metal ion. The Zn^{II}-binding affinity of **HS** can also be demonstrated by the conditional stability calculated at pH 7.4 and 1 : 1 metal ion to ligand ratio based on the equations below,

$$H_qL + Zn \rightleftarrows ZnH_qL$$

$$K_a = \frac{[ZnH_qL]}{[Zn][H_qL]}$$

where Zn denotes the free Zn^{II} concentration while H_qL and ZnH_qL represent the overall concentration of the free and complexed ligands in any protonation states, respectively. The apparent stability constant for the above conditions is K_a = 7.5 × 10^7 ($\log K_a$ = 7.9) which is in the lower range of affinities reported for various wild-type bacterial Zn^{II}-regulators[64] or variants.[65]

The deprotonation of ZnL above pH ~ 8 (Fig. 6A) leads to the species $ZnH_{-1}L$ being strongly dominant under alkaline conditions. The observed extra deprotonation is most likely not a ligand-related proton release since the formation of a Zn^{II}–amide bond is a very scarce event in the complexes of Zn^{II} formed with terminally protected peptides.[62,66–69] Accordingly, the $ZnH_{-1}L$ composition may represent a species with a deprotonated water ligand, described as Zn(OH)L. The pK_a value of the deprotonation process is 8.65 that is *ca.* 1.7 log units lower than the pK_a determined for the same type of proton release of the Cd^{II} complex of **HS**,[13] as expected, due to the smaller ionic radius of Zn^{II} as compared to Cd^{II}. The deprotonation of the bound H_2O occurs also at a somewhat lower pH than in the ZnL complex of a similar ligand containing no His residue in position 3 of the peptide chain (pK_a = 9.11[50]). The $\{Zn(Cys)_2HisH_2O/OH^-\}$ coordination sphere is also found in horse liver alcohol dehydrogenase (LADH), where the pK_a of the metal ion bound water molecule is 9.2 for the native Zn^{II} containing enzyme,[70] and 11.0 for the Cd^{II} substituted species.[71] Interestingly, the pK_a of the Zn^{II}-bound water is lower in **HS** than in LADH. It seems that above neutral pH the histidine of **HS** significantly influences speciation, the coordination sphere of Zn^{II} and even the peptide structure, as indicated by UV and SRCD data.

Monomeric ZnHL and ZnL complexes dominate in the acidic/neutral pH-range when **HS** is present in a twofold excess over Zn^{II} (Fig. 6B). As indicated by UV data, metal-bridged bis-ligand species with different protonation states are also formed above pH ~ 6. Although the determined stabilities of the various bis-complexes do not provide direct information on the binding mode of the ligands, the relatively high pK_a value for the $ZnHL_2 \rightarrow ZnL_2 + H^+$ process (= 8.7, Table 2) suggests that there are protonated thiol groups in the ZnH_2L_2 and $ZnHL_2$ species. The stability constant calculated for the binding of the second ligand in ZnL_2 ($\log K_2$ = 4.37) and the relative stability of the parent mono- and bis-complexes ($\log(K_1/K_2)$ = 6.26) shows a notably weaker binding of the second ligand as compared to the same process in the Cd^{II} : **HS** system ($\log(K_1/K_2)$ = 5.33 [13]) or to the Zn^{II}-binding of the above cited His-free peptide ($\log(K_1/K_2)$ = 5.14 [50]). This finding provides a further support for the important role of histidine in controlling the interaction of Zn^{II} with **HS**.

^{1}H NMR experiments

Assignment of the ^{1}H NMR resonances of **HS** and the pH-dependence of the recorded spectra in the absence of metal ions were published previously.[13] Hg^{II} coordination to the peptide has a strong effect on the resonances of the Cys $C_\beta H_2$ protons (Fig. 7). These signals shift from 2.93 ppm to relatively broad peaks at ~3.3–3.4 ppm (in an accidental overlap with one of the His $C_\beta H_2$ resonances at pH 4.0–6.0) in the presence of one equivalent of Hg^{II}. The significant, *ca.* 0.4 ppm downfield shift of the Cys $C_\beta H_2$ resonances of the bound ligand, as compared to the same signals of the free **HS** indicates the binding of both thiolates to the metal ion, as also suggested by UV titrations.

Two separate signal sets of the Cys $C_\beta H_2$ protons are observed at pH 4.0–6.0 when **HS** is in a twofold excess over Hg^{II} (Fig. 7) One set is reminiscent of the resonances of the free ligand, whereas the other coincides with those observed in the Hg^{II} : **HS** 1 : 1 system. Increasing pH to 8.0 results in coalescence of the two signal sets to a very broad bulge-like feature in the range of δ ~ 2.8–3.4 ppm overlapping with the His $C_\beta H_2$ resonances (Fig. 7). This coalesced signal, with a chemical shift found in between those observed for Hg^{II} : **HS**

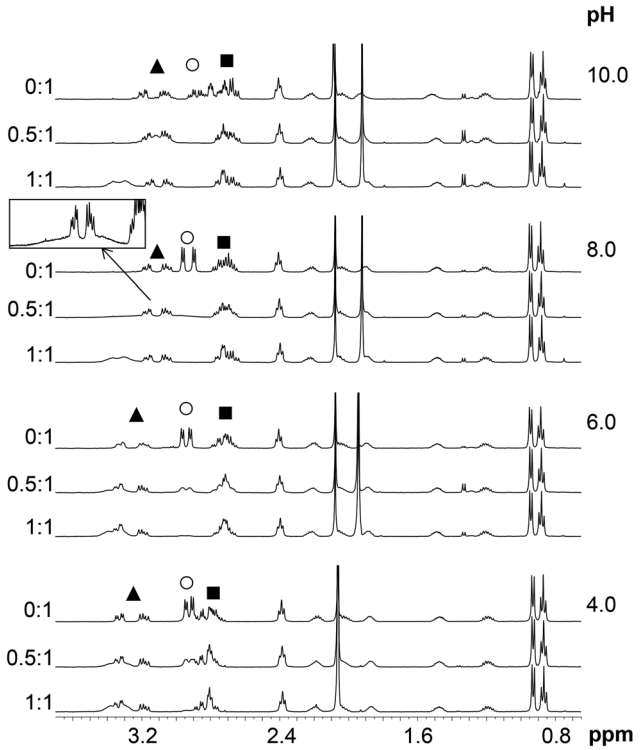

Fig. 7 Selected regions of the ^{1}H NMR spectra of **HS** recorded in the absence and presence of 0.5 and 1.0 eq. of Hg^{II} (H_2O/D_2O = 90 : 10% v/v, c_{HS} = 1.3 × 10^{-3} M, T = 298 K). The resonances marked by symbols are: His $C_\beta H_2$: ▲; Cys $C_\beta H_2$: ○; Asp $C_\beta H_2$: ■. The region of δ = 2.7–3.6 ppm from the Hg^{II} : **HS** 0.5 : 1 spectrum at pH = 8.0 is magnified in the frame. Note that the sharp signals at $\delta \sim 1.9$ ppm are those of the acetate anion of the added mercury(II) salt which coincide with the acetyl protecting group resonances of **HS** at pH ~ 4.0.

1 : 1 and the free ligand, becomes sharper on increasing pH but is still broad at pH = 10.0. These findings indicate that the ligand exchange rate between the free and bound forms gradually increases from the slow/intermediate to the intermediate/fast time regime in parallel with the deprotonation of the unbound thiol groups of the presumably free ligand being present in the Hg^{II} : **HS** 0.5 : 1 system.

The exchange rate, k_{ex}, between the bound and non-bound ligand forms may be roughly estimated from the observed line-broadening[72] at pH 4.0–6.0 which is dominated by slow exchange. The line-broadening, w_e–w_0, occurring for the Cys $C_\beta H_2$ resonances of the free peptide due to the addition of 0.5 eq. Hg^{II} is *ca.* 12 Hz which leads to $k_{ex} \sim \pi \times (w_e - w_0) \sim 38\ s^{-1}$ at pH = 6.0 (w_e and w_0 represent the line width of signals at half height with and without exchange, respectively). The calculation is based on the assumption of a two-site exchange of **HS** between a specific Hg^{II}-peptide bound form and the non-bound form under the applied experimental conditions. k_{ex} may also be expressed by a formulae involving the rates of the association and dissociation processes, as follows[73]

$$k_{ex} = k_{on}[M] + k_{off} = \frac{k_{off}}{1-f}$$

where k_{on} and k_{off} stands for the second order rate constant of the complex formation and the first order rate constant of the complex dissociation, respectively, [M] is the concentration of the metal ion and f represents the bound fraction of the ligand (0.5 in the present case). If one assumes that the association is diffusion controlled and thus $k_{on} \sim 7.4 \times 10^9\ M^{-1}\ s^{-1}$ that is the rate constant for diffusion controlled reactions in water at 298 K,[74] solving the above equation for [M] would result in a concentration of [Hg^{II}] that corresponds to a $K_d \sim 2.5 \times 10^{-9}$ M dissociation constant of the complex at pH = 6.0. This K_d value suggests a many orders of magnitude weaker binding than expected for a typical {HgS_2} complex,[41] indicating that the picture is too simplistic, and presumably a more complex speciation occurs.

The increase of pH also induces the upfield shift of the resonances of the Asp ($C_\beta H_2$ protons – Fig. 7) and His ($C_\beta H_2$ – Fig. 7 and the $C_{\varepsilon 1}H$ and $C_{\delta 2}H$ protons of the imidazole ring – Fig. 8) reflecting the deprotonation of the side chains of these residues. The chemical shift values are practically independent of the metal ion to ligand ratio at all selected pH values. These findings indicate that the proton releases from the Asp carboxyl groups and the His imidazole moiety are practically unaffected by the presence of Hg^{II} and therefore that these groups do not participate in Hg^{II}-binding. Nevertheless, coordination of the cysteine residues to Hg^{II} has a slight line

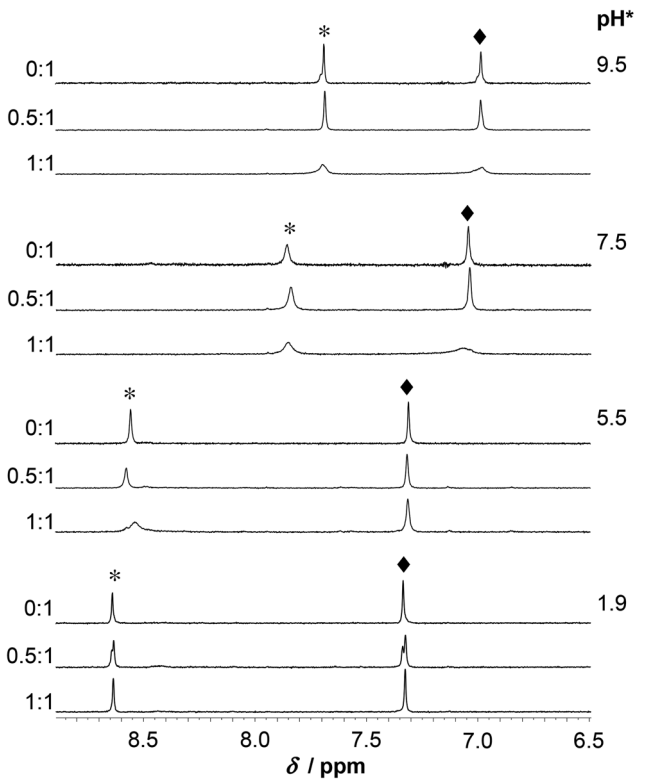

Fig. 8 Part of the ^{1}H NMR spectra of the peptide **HS** recorded at various pH* values in D_2O as a function of the Hg^{II} to peptide ratio (c_{HS} = 1.3 × 10^{-3} M, T = 298 K). The symbols denote the $C_{\varepsilon 1}H$ (*) and $C_{\delta 2}H$ (◆) resonances of His.

width increasing effect on the neighbouring Asp side chain resonances under acidic conditions (Fig. 7) and a rather pronounced impact on the His $C_{\varepsilon 1}H$ and $C_{\delta 2}H$ signals in neutral/alkaline solutions (Fig. 8). This shows that although the chemical shifts, apart from those of the cysteines, do not change significantly, the dynamics of the peptide is affected by the binding of Hg^{II}.

The spectra of **HS** obtained at pH ~ 4.4 in the presence and absence of Zn^{II} reflect no differences either in terms of the chemical shifts or the shape of the various ^{1}H-resonances (Fig. S7†). This suggests that, as opposed to Hg^{II}, Zn^{II} is not bound to **HS** under such conditions, which is in agreement with the potentiometric and UV absorption studies, *vide supra*. At pH ~ 5.5, however, the presence of Zn^{II} gives rise to pronounced broadening of most resonances. In the presence of 0.5 eq. Zn^{II} this may indicate exchange between the bound and free states of the peptide, but in the fully loaded Zn^{II}:**HS** system it implies equilibria between conformers falling into the intermediate exchange time regime (ms–s) (Fig. 9–10). At a 1 : 1 ratio of Zn^{II} and **HS** the $C_{\varepsilon 1}H$ and $C_{\delta 2}H$ signals of the His imidazole are shifted slightly upfield as compared to the resonances of the free ligand (Fig. 10). At 0.5 eq. of Zn^{II} the chemical shifts of the imidazole ring protons appear in between those of the free **HS** and the 1 : 1 system reflecting an equilibrium between the non-bound and metal-bound peptide forms, and fast exchange dynamics for these resonances. The $C_{\varepsilon 1}H$ and $C_{\delta 2}H$ resonances are significantly shifted upfield by a further pH increase (pH 5.5 → 7.0), similarly to the metal ion free solution, which indicates that His-coordination is not completed at pH 5.5. A combined interpretation of the ^{1}H NMR, UV absorption, and potentiometric data at pH ~ 5.5, (see Fig. 6) leads us to propose co-existing binding isomers of the ZnHL species, with the participation of two Cys-thiolates or one of the Cys-thiolates and the His side chain in metal ion binding.

The increase of pH to pH ~ 7.0 gives rise to a substantial change of the spectral pattern. According to our data, all the metal ions are complexed under such conditions (Fig. 6). Most of the resonances, in addition to those of the Cys residues, display line broadening, in contrast to the signals observed for Hg^{II}:**HS**, where resonances from non-coordinating groups are not affected to the same extent. Thus, Zn^{II}-coordination affects the internal dynamics of the entire peptide on the NMR time scale. Additionally, the ligand exchange dynamics is slowed down to the moderately slow exchange time regime causing the splitting of several ^{1}H resonances ($C_\beta H_2$, $C_{\varepsilon 1}H$ and $C_{\delta 2}H$ of His and all the resonances of Ile) into clearly distinguishable separate signals at a 0.5 : 1 Zn^{II}:**HS** ratio (see spectra at pH ≥ 7.0 on Fig. 9–10). The decrease of exchange rate by pH-increase coincides with a remarkable change of the CD-signals (Fig. 4), and occurs in parallel with the formation of the ZnL parent complex. It implies that the participation of several donor groups in metal ion binding leads to a reduced lability of species. At a 1 : 1 Zn^{II}:**HS** ratio, the $C_\beta H_2$ protons of the Cys and His residues experience a significant chemical shift change relative to the free ligand, as do the $C_{\varepsilon 1}H$ and $C_{\delta 2}H$

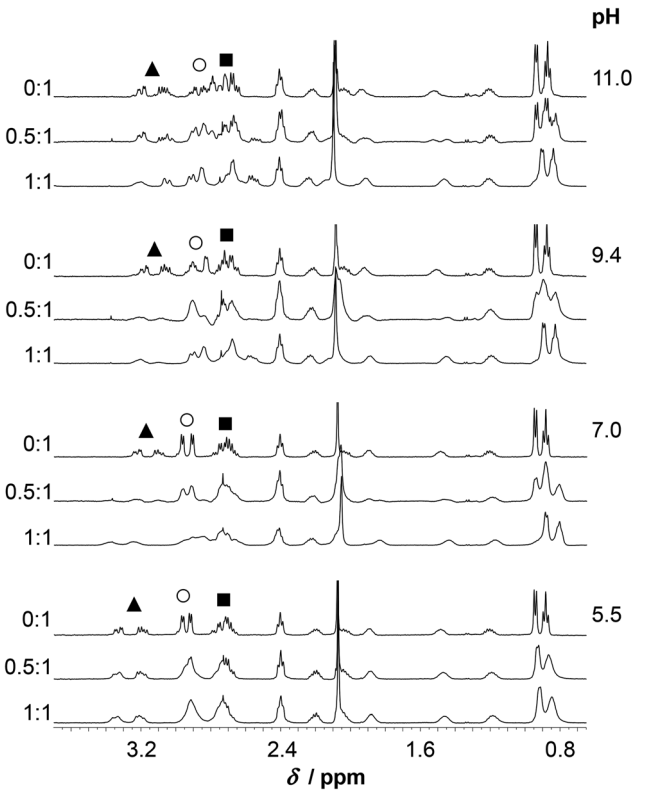

Fig. 9 Aliphatic region of the ^{1}H NMR spectra of **HS** recorded in the absence of Zn^{II} and in the Zn^{II}:**HS** 0.5 : 1 and 1 : 1 systems (H_2O/D_2O = 90 : 10% v/v, $c_{HS} = 1.3 \times 10^{-3}$ M, T = 298 K). $C_\beta H_2$ resonances of the residues with potential donor groups are indicated by the following symbols: His $C_\beta H_2$: ▲; Cys $C_\beta H_2$: ○; Asp $C_\beta H_2$: ■.

signals of the imidazole ring (Fig. 10). This supports the coordination of the two Cys-thiolates and the His-imidazole groups to Zn^{II} in ZnL, but the poorly resolved spectrum at pH = 7.0 does not provide information on the binding of Asp-carboxylates. As pointed out above, various resonances of the C-terminal Ile residue in the spectral region 0.8–1.0 ppm ($C_\delta H_3$, $C_{\gamma 2}H_3$) are also strongly affected by metal ion coordination as those of the bound ligand are clearly shifted upfield compared to the ones of the free peptide-like resonances (Zn^{II}:**HS** 0.5 : 1, Fig. 9). Analogous spectral features were not observed in the systems of either Cd^{II} and **HS**[13] or Zn^{II} and a closely related peptide[50] differing only in the His-residue from the presently studied ligand. Thus, while the exact origin of the impact of Zn^{II}-binding on the Ile resonances is not clear, metal ion coordination of the histidine unit very likely plays a key role here.

Based on the observed line broadening of the Cys $C_\beta H_2$ protons at Zn^{II}:**HS** 0.5 : 1 (Fig. 9) a similar or slightly lower exchange rate between the bound and non-bound ligands, as compared to Hg^{II}:**HS**, may be predicted. However, the overlap of the various resonances and the complexity of the system (see the distribution curves at pH ~ 7.0, Fig. 6B) do not allow a deeper discussion. It is, however, an interesting contrast to Hg^{II}:**HS**, that the exchange rate in the presence of Zn^{II}

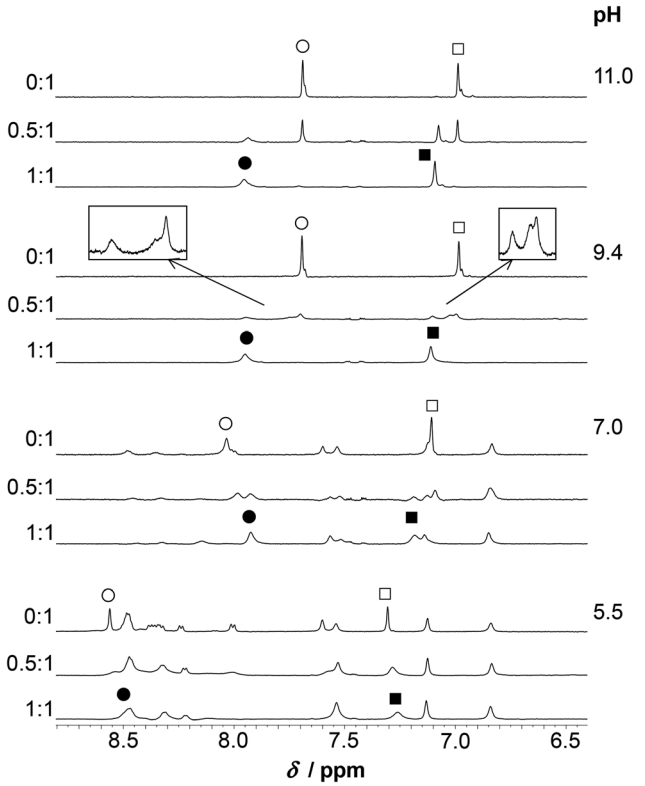

Fig. 10 Aromatic/H_N region of the ^{1}H NMR spectra of **HS** recorded in the absence of Zn^{II} and in the Zn^{II} : **HS** 0.5 : 1 and 1 : 1 systems (H_2O/D_2O = 90 : 10% v/v, c_{HS} = 1.3 × 10^{-3} M, T = 298 K). The open circle and square symbols show resonances of the non-bound ligand ($C_{\varepsilon 1}H$ and $C_{\delta 2}H$, respectively) while the filled symbols mark the same resonances of the bound His residues in the mononuclear species. The regions of δ = 6.9–7.15 and 7.4–8.05 ppm from the Zn^{II} : **HS** 0.5 : 1 spectrum at pH ~ 9.4 are magnified in the frames.

remains relatively slow even at higher pH (see below) approaching the deprotonation-range of the thiol groups of the free ligand. The increased metal ion exchange rate, as observed by the resonances of the Cys $C_\beta H_2$ protons (see Fig. 7) with 0.5 eq. Hg^{II} for pH above the pK_a of the thiols, imply that the free thiolates take part in the exchange process, and thus that it occurs *via* an associative mechanism. The low coordination number may be important for this process, as it may allow for coordination of additional thiolates in the equatorial plane. This is analogous to a proposed mechanism of transfer of Cu^I between proteins,[42,75,76] where the metal ion is also found in a structure with two thiolates coordinating. Contrary to this, the metal exchange rate does not change into the fast exchange regime with 0.5 eq. Zn^{II} for pH above the pK_a for the thiols, see Fig. 9. This may reflect that the exchange occurs *via* a dissociative mechanism, although not necessarily *via* free Zn^{II}, in analogy to the common interpretation of ligand binding reactions for the Zn^{II} aqua ion involving dissociation of coordinated water as the rate determining step.[77]

As a conclusion, and in line with SRCD data, the simultaneous binding of (at least) three side chain donors induces a more defined ligand structure in the Zn^{II}-bound **HS**, unlike the loop-like conformation proposed for Hg^{II} : **HS**.

At pH ~ 9.4 the spectra of the Zn^{II}-containing solutions are still very poorly resolved as the resonances are strongly broadened. Coordination of His to the metal ion in the Zn^{II} : **HS** 1 : 1 system is unambiguously demonstrated by the significant downfield shift of the $C_{\varepsilon 1}H$ and $C_{\delta 2}H$ resonances, as compared to the metal ion free sample (Fig. 10). A similar shift was observed and attributed to His-coordination in the Cd^{II}-complex of the peptide.[13] At least three distinguishable, broad $C_{\delta 2}H$ peaks and three $C_{\varepsilon 1}H$ peaks, albeit less clearly, are observed at 0.5 : 1 Zn^{II} : peptide ratio (see the enlarged spectrum segments on Fig. 10). One of the $C_{\delta 2}H$ and $C_{\varepsilon 1}H$ peaks appear very close to the free ligand-like signals while the third observed signals have chemical shifts resembling those measured for the 1 : 1 system. In order to elucidate the processes occurring in the presence of ligand excess above neutral pH, a more detailed series of spectra were recorded at pH ~ 8. One may follow the evolution of the $C_{\varepsilon 1}H$ and $C_{\delta 2}H$ signals from 0 : 1 to 1 : 1 Zn^{II} : peptide ratio on Fig. 11. The series describe the complete transformation of the non-bound ligand to the 1 : 1 species (mostly ZnL at this pH, see Fig. 6A). The spectra recorded at the intermediate stages, featuring the emergence and transformation of broad peaks, originate from a dynamic exchange between at least three coexisting species (see *e.g.* the $C_{\varepsilon 1}H$ resonances at a Zn^{II} : **HS** ratio of 0.75 : 1 or the $C_{\delta 2}H$ resonances at a ratio of 0.5 : 1), the free peptide, the fully loaded Zn^{II}-peptide complex, and a species with a plausible 0.5 : 1 Zn^{II} : **HS** stoichiometry, *i.e.* a bis-ligand complex.

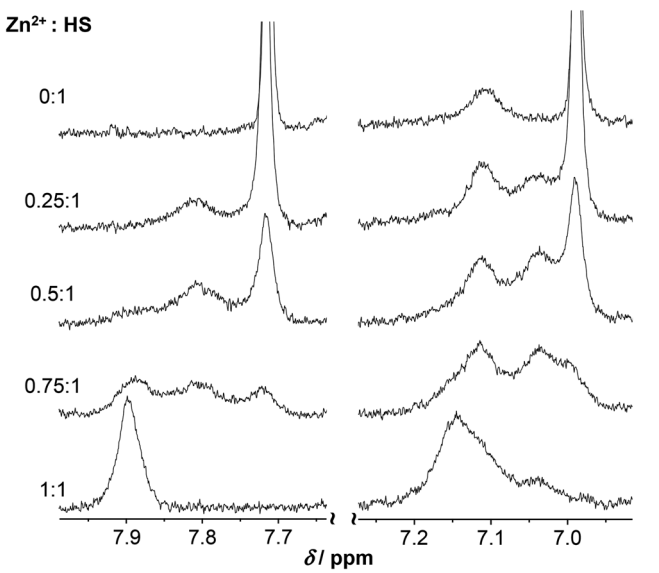

Fig. 11 Part of the ^{1}H NMR spectra of **HS** recorded at pH ~ 8.0 as a function of the metal ion to peptide ratio (H_2O/D_2O = 90 : 10% v/v, c_{HS} = 1.3 × 10^{-3} M, T = 298 K). The selected regions reveal changes observed on the $C_{\varepsilon 1}H$ (left) and $C_{\delta 2}H$ (right) resonance of the His-imidazole moiety of the ligand. Note that the peak seen at δ ~ 7.11 ppm on the free **HS** spectrum is one of the remaining amide resonances still observable at pH ~ 8.0.

This provides strong support for the potentiometric data. The species are in slow to intermediate exchange rate relative to the NMR timescale. The emerging signals in the range of $\delta \sim$ 7.0–7.08 and 7.75–7.85 ppm suggests that the His-imidazole moiety of at least one of the two ligands plays a role in Zn^{II}-coordination in some or all of the bis-complexes.

Only two sets of relatively sharp $C_{\varepsilon 1}H$ and $C_{\delta 2}H$ resonances are detected at pH ~ 11 in the Zn^{II} : **HS** 0.5 : 1 system (Fig. 10) which is in excellent correlation with the equilibrium and UV results, *i.e.* the presence of only the $ZnH_{-1}L$ complex and free ligand. Besides, the notable chemical shift changes observed on the spectra of Zn^{II} : **HS** 1 : 1 from pH ~ 7.0 up to 11.0 (see *e.g.* the range of $\delta \sim$ 3.5–2.5 ppm (Fig. 9) or the $C_{\delta 2}H$ signals (Fig. 10), clearly reflect the conversion of the ZnL parent complex to $ZnH_{-1}L$.

Conclusion

The 12-mer **HS** peptide, inspired by the C-terminal metal ion binding domain of a bacterial metalloregulator CueR, is shown to efficiently bind Hg^{II} and Zn^{II}, two metal ions with significantly different coordination preferences. Hg^{II} is demonstrated to form a loop-like structure in a $\{HgS_2\}$ coordination fashion *via* binding to the two cysteinates of the ligand, but there is no sign for the participation of any other side chain donors in Hg^{II}-coordination. The kinetic lability of Hg^{II} is manifested in line broadening on the ^{1}H NMR spectra affecting mostly the resonances of the bound Cys residues and those of the neighbouring units. In contrast to Hg^{II}, Zn^{II} dictates the peptide to a more structured form in its ZnL complex *via* binding to at least three side chain donors, the two Cys thiolates and the His imidazole. Indeed, the SRCD spectra above neutral pH might reflect an increasing helical content in the Zn^{II}-bound **HS**, although a contribution of the thiolate–metal ion chromophore to the observed CD-pattern may also be present in the same wavelength range. In addition to monomeric species, bis-ligand **HS**-Zn^{II}-**HS** complexes are also formed, unlike with Hg^{II}. The line broadening in ^{1}H-NMR is pronounced for most of the resonances, indicating that exchange dynamics between different conformers occurs on the NMR time scale (ms–s) and that, in contrast to Hg^{II}, Zn^{II}-coordination notably affects the internal dynamics of the entire peptide chain. The results obtained demonstrate that the conformational and coordination flexibility allows **HS** to adopt diverse structures, favoured by different metal ions, which is a property that may be utilized for metal ion sequestration in practical applications. Experimental studies on the interaction of a flexible peptide like **HS** with metal ions are a challenge as speciation may be diverse and the system dynamic. In the span between coordination compounds to metalloproteins, dynamic systems like **HS**, may yield insight into the underlying mechanisms of metal ion exchange that are necessary to account for transport and distribution of essential trace elements in biological systems. In a more fundamental perspective, also the potential role of metal ions for protein folding (and misfolding) through transient binding may also be elucidated by interrogating such peptide–metal ion interactions.

Experimental

Materials

The investigated peptide *N*-acetyl-Ser-Cys-His-Gly-Asp-Gln-Gly-Ser-Asp-Cys-Ser-Ile-NH_2 (Ac-SCHGDQGSDCSI-NH_2, **HS**) was synthesized, as described earlier.[13] Chemicals and solvents were obtained from Sigma-Aldrich and used without further purification unless otherwise described. The solutions of $Zn(ClO_4)_2 \cdot nH_2O$, $Hg(OAc)_2$ (Aldrich) were standardized complexometrically[78] while precise weights of high purity $HgCl_2$ (Aldrich) was used to prepare metal ion stock solutions. pH-Metric titrations were performed with NaOH (Aldrich) solutions standardized using potassium hydrogen phthalate (Sigma-Aldrich).

Electronic absorption and SRCD measurements

UV–Visible (UV–Vis) spectra were measured on a Shimadzu UV-3600 UV-VIS-NIR spectrophotometer using a cell with 1 cm optical pathlength. Concentration of the ligand was 1.0×10^{-4} M and the metal ion concentration varied between 5.0×10^{-5} and 2.0×10^{-4} M.

The synchrotron radiation CD (SRCD) spectra of the free ligand and the metal complexes were recorded at the SRCD facility at the CD1 beamline on the storage ring ASTRID at the Institute for Storage Ring Facilities (ISA), University of Aarhus, Denmark.[79,80] All spectra were recorded with 1 nm steps and a dwell time of 2 s per step, using 0.1 mm quartz cells (SUPRASIL, Hellma GmbH, Germany), for the wavelength range of 175–260 nm. The substances were initially dissolved in 1.0×10^{-2} M HCl in order to avoid the eventual oxidation process. The pH of the samples ($c_{peptide} = 1.0 \times 10^{-3}$ M) were adjusted by adding the appropriate amount of NaOH solution. From the raw spectra the water baseline was subtracted and spectra were normalized to 1.0×10^{-3} M peptide concentration (to eliminate the effect of dilution).

Perturbed angular correlation of γ-rays

All perturbed angular correlation (PAC) experiments were performed in ISOLDE/CERN with a setup using six BaF_2 detectors keeping the samples at a temperature of 1 °C. Production and purification of the radioactive ^{199m}Hg is described in the literature.[81] The ^{199m}Hg solution (150 μL) was mixed with solutions of nonradioactive mercury(II) chloride, sodium perchlorate and buffer if needed. TRIS and CAPS buffers were used for adjusting the pH of samples to pH ~ 8.0 and 10, respectively. The peptide was dissolved in 0.01 M perchloric acid and amounts of this stock solution were added to the buffered Hg^{II}-containing solutions to reach the desired final concentrations. Finally, sucrose was added to 55% w/w. The pH of the solutions was adjusted with NaOH and $HClO_4$. In order to avoid contamination of the samples, small volumes were taken for pH

measurements. The temperature dependence of the pH in the TRIS/CAPS-buffered solutions was taken into account and pH-values were corrected to 1 °C.[82] The buffers and the peptide stock solutions were purged with argon. The final volume of the samples was 210 μL with $c_{peptide} = c_{Hg^{II}} = 8.03 \times 10^{-5}$ M and $c_{buffer} = 1.60 \times 10^{-2}$ M.

NMR experiments

^{1}H NMR measurements were performed on a Bruker Avance DRX 500 spectrometer operating at 500.132 MHz. The spectra were recorded at $T = 298$ K in a mixture of $H_2O/D_2O = 90:10\%$ v/v and in a few cases in pure D_2O applying the zgpr or zgcppr pulse sequences in order to presaturate the H_2O/HDO resonances. In a typical sample the concentration of the peptide was 1.3×10^{-3} M. The chemical shifts were referenced to TSP-d4 at 0.0 ppm. Spectra were recorded using a recycle delay of 5 s, an acquisition time of 1.64 s, a spectral width of 5 or 10 kHz and 64–128 scans. In D_2O, the pH* (pH-meter reading uncorrected by the deuterium effect) was adjusted to the desired values with NaOD. The recorded spectra were processed by the ACD/Spectrus Processor software.[83]

pH-Potentiometric measurements

The protonation and coordination equilibria were investigated in aqueous solutions ($I = 0.1$ M $NaClO_4$, and $T = 298.0 \pm 0.1$ K) under argon atmosphere with a special care to avoid the oxidation of the peptide. The potentiometric titrations were carried out by an automatic titration set including a PC controlled Dosimat 665 (Metrohm) autoburette, an Orion 710A precision digital pH-meter equipped with an Orion 8103BNUWP Ross Ultra semi micro pH electrode (165 × 6 mm). Conversion of the relative mV values as pH-meter readings to hydrogen ion concentrations was done as described earlier.[50] The protonation and complex formation processes were characterized by the following general equilibrium process:

$$pM + qH + rL \rightleftarrows M_pH_qL_r$$

$$\beta_{M_pH_qL_r} = \frac{[M_pH_qL_r]}{[M]^p[H]^q[L]^r}$$

where M denotes the metal ion, L the deprotonated ligand molecule, and H the protons. Charges have been omitted for simplicity but can be easily calculated taking into account the composition of the fully protonated dodecapeptide (H_5L^+). Please note, that this simplified notion is used generally throughout the text and on the figures. The corresponding formation constants ($\beta_{M_pH_qL_r} \equiv \beta_{pqr}$) were calculated using the PSEQUAD computer program.[84] The protonation constants were determined from 3–4 independent titrations (70–80 data points per titration), with a peptide concentration of 1.0×10^{-3} M. The complex formation constants were evaluated from 8 independent titrations (70–80 data points per titration). The applied ratio of Zn^{II} and the ligand was 0.5 : 1, 1 : 1 and 2 : 1 with the Zn^{II} concentration varied between 5.2×10^{-4} and 2.04×10^{-3} M. Due to precipitation in the presence of metal ion excess in alkaline pH-range, titration data for the Zn^{II} : **HS** 2 : 1 samples were evaluated only up to pH 7.1. (The individual fitting parameter of titrations performed with ligand excess dropped by *ca.* 40% when considering differently protonated bis-ligand species (ZnH_xL_2) besides monomeric ones, and accordingly such species were also included in the final model.

Acknowledgements

AJ wishes to thank the financial support of the János Bolyai Research Grant from the Hungarian Academy of Sciences. The research leading to the SRCD results has received funding from the European Community's Seventh Framework CALIPSO Programme (FP7/2007–2013, grant No. 312284). LH was supported by ISOLDE/CERN by the beam time grant IS488.

References

1 D. P. Giedroc and A. I. Arunkumara, *Dalton Trans.*, 2007, 3107.
2 Z. Ma, F. E. Jacobsen and D. P. Giedroc, *Chem. Rev.*, 2009, **109**, 4644.
3 K. J. Waldron, J. C. Rutherford, D. Ford and N. J. Robinson, *Nature*, 2009, **460**, 823.
4 K. J. Waldron and N. J. Robinson, *Nat. Rev. Microbiol.*, 2009, **6**, 25.
5 B. Zambelli, F. Musiani and S. Ciurli, *Metal Ion-Mediated DNA-Protein Interactions in Interplay between Metal Ions and Nucleic Acids, Metal Ions in Life Sciences 10*, ed. A. Sigel, H. Sigel and R. K. O. Sigel, Springer, Netherlands, 2012, pp. 135–170.
6 N. L. Brown, J. V. Stoyanov, S. P. Kidd and J. L. Hobman, *FEMS Microbiol. Rev.*, 2003, **27**, 145.
7 J. L. Hobman, J. Wilkie and N. L. Brown, *BioMetals*, 2005, **18**, 429.
8 A. Changela, K. Chen, Y. Xue, J. Holschen, C. E. Outten, T. V. O'Halloran and A. Mondragon, *Science*, 2003, **301**, 1383.
9 M. Mejáre and l. Bülow, *Trends Biotechnol.*, 2001, **19**, 67.
10 M. Valls and V. de Lorenzo, *FEMS Microbiol. Rev.*, 2002, **26**, 327.
11 K. Kuroda and M. Ueda, *Curr. Opin. Biotechnol.*, 2011, **22**, 427.
12 K. D. Brune and T. S. Bayer, *Front. Microbiol.*, 2012, **3**, 1.
13 A. Jancso, D. Szunyogh, F. H. Larsen, P. W. Thulstrup, N. J. Christensen, B. Gyurcsik and L. Hemmingsen, *Metallomics*, 2011, **3**, 1331.
14 D. S. Auld, Zinc enzymes, in *Encyclopedia of Inorganic and Bioinorganic Chemistry*, John Wiley & Sons, Ltd., 2011, DOI: 10.1002/9781119951438.eibc0241.
15 M. A. Pennella and D. P. Giedroc, Zinc: DNA Binding Proteins, in *Encyclopedia of Inorganic and Bioinorganic*

Chemistry, John Wiley & Sons, Ltd., 2011, DOI: 10.1002/9781119951438.eibc0240.
16 I. Dokmanic, M. Sikic and S. Tomic, *Acta Crystallogr., Sect. D: Biol. Crystallogr.*, 2008, **64**, 257.
17 M. Laitaoja, J. Valjakka and J. Jänis, *Inorg. Chem.*, 2013, **52**, 10983.
18 D. S. Auld, *BioMetals*, 2001, **14**, 271.
19 M. J. Stillman, *Coord. Chem. Rev.*, 1995, **144**, 461.
20 S. S. Krishna, I. Majumdar and N. V. Grishin, *Nucleic Acids Res.*, 2003, **31**, 532.
21 R. Gamsjaeger, C. K. Liew, F. E. Loughlin, M. Crossley and J. P. Mackay, *Trends Biochem. Sci.*, 2007, **32**, 63.
22 D. C. Bebout, Mercury: Inorganic & Coordination Chemistry, in *Encyclopedia of Inorganic and Bioinorganic Chemistry*, John Wiley & Sons, Ltd., 2011, DOI: 10.1002/9781119951438.eibc0124.
23 A. Manceau and K. L. Nagy, *Dalton Trans.*, 2008, 1421.
24 M. Kaupp and H. G. von Schnering, *Inorg. Chem.*, 1994, **33**, 2555.
25 J. G. Wright, M. J. Natan, F. M. MacDonnell, D. M. Ralston and T. V. O'Halloran, Mercury(II)-Thiolate chemistry and the mechanism of the heavy metal biosensor MerR, in *Progress in Inorganic Chemistry: Bioinorganic Chemistry*, ed. S. J. Lippard, John Wiley & Sons, New York, 1990, vol. 38, pp. 323–412.
26 D. L. Huffman, L. M. Utschig and T. V. O'Halloran, Mercury-responsive gene regulation and mercury-199 as a probe of protein structure, in *Metal Ions in Biological Systems*, ed. A. Sigel and H. Sigel, Marcel Dekker, New York, 1997, vol. 34, pp. 503–526.
27 R. A. Steele and S. J. Opella, *Biochemistry*, 1997, **36**, 6885.
28 J. G. Wright, H.-T. Tsang, J. E. Penner-Hahn and T. V. O'Halloran, *J. Am. Chem. Soc.*, 1990, **112**, 2434.
29 J. D. Helmann, B. T. Ballard and C. T. Walsh, *Science*, 1990, **247**, 946.
30 L. M. Utschig, T. Baynard, C. Strong and T. V. O'Halloran, *Inorg. Chem.*, 1997, **36**, 2926.
31 P. Faller, B. Ctortecka, W. Tröger, T. Butz and M. Vasák, *J. Biol. Inorg. Chem.*, 2000, **5**, 393.
32 U. Heinz, L. Hemmingsen, M. Kiefer and H.-W. Adolph, *Chem. – Eur. J.*, 2009, **15**, 7350.
33 M. Vasak, J. H. Kagi and H. A. Hill, *Biochemistry*, 1981, **20**, 2852.
34 J. H. Kägi, M. Vasák, K. Lerch, D. E. Gilg, P. Hunziker, W. R. Bernhard and M. Good, *Environ. Health Perspect.*, 1984, **54**, 93.
35 L. M. Utschig, J. G. Wright and T. V. O'Halloran, Biochemical and Spectroscopic Probes of Hg(II) Coordination Environments in Proteins, in *Methods in Enzymology*, ed. B. Vallee and J. Riordan, Academic Press, Inc., San Diego, CA, 1993, vol. 226, pp 71–97.
36 N. A. Rey, O. W. Howarth and E. C. Pereira-Maia, *J. Inorg. Biochem.*, 2004, **98**, 1151.
37 A. Kolozsi, A. Lakatos, G. Galbács, A.Ø. Madsen, E. Larsen and B. Gyurcsik, *Inorg. Chem.*, 2008, **47**, 3832.
38 G. R. Dieckmann, D. K. McRorie, D. L. Tierney, L. M. Utschig, C. P. Singer, T. V. O'Halloran, J. E. Penner-Hahn, W. F. DeGrado and V. L. Pecoraro, *J. Am. Chem. Soc.*, 1997, **119**, 6195.
39 P. Rousselot-Pailley, O. Seneque, C. Lebrun, S. Crouzy, D. Boturyn, P. Dumy, M. Ferrand and P. Delangle, *Inorg. Chem.*, 2006, **45**, 5510.
40 A. M. Pujol, C. Lebrun, C. Gateau, A. Manceau and P. Delangle, *Eur. J. Inorg. Chem.*, 2012, 3835.
41 S. Pires, J. Habjanic, M. Sezer, C. M. Soares, L. Hemmingsen and O. Iranzo, *Inorg. Chem.*, 2012, **51**, 11339.
42 M. Łuczkowski, B. A. Zeider, A. V. H. Hinz, M. Stachura, S. Chakraborty, L. Hemmingsen, D. L. Huffman and V. L. Pecoraro, *Chem. – Eur. J.*, 2013, **19**, 9042.
43 O. Iranzo, D. Ghosh and V. L. Pecoraro, *Inorg. Chem.*, 2006, **45**, 9959.
44 M. Łuczkowski, M. Stachura, V. Schirf, B. Demeler, L. Hemmingsen and V. L. Pecoraro, *Inorg. Chem.*, 2008, **47**, 10875.
45 E.-D. Ciuculescu, Y. Mekmouche and P. Faller, *Chem. – Eur. J.*, 2005, **11**, 903.
46 U. Heinz, M. Kiefer, A. Tholey and H.-W. Adolph, *J. Biol. Chem.*, 2005, **280**, 3197.
47 Y. Cheng, Y.-B. Yan and J. Liu, *J. Inorg. Biochem.*, 2005, **99**, 1952.
48 R. Kobayashi and E. Yoshimura, *Biol. Trace Elem. Res.*, 2006, **114**, 313.
49 T. Kochanczyk, P. Jakimowicz and A. Krezel, *Chem. Commun.*, 2013, **49**, 1312.
50 A. Jancso, B. Gyurcsik, E. Mesterhazy and R. Berkecz, *J. Inorg. Biochem.*, 2013, **126**, 96.
51 N. Greenfield and G. D. Fasman, *Biochemistry*, 1969, **8**, 4108.
52 A. Lombardi, D. Marasco, O. Maglio, L. Di Costanzo, F. Nastri and V. Pavone, *Proc. Natl. Acad. Sci. U. S. A.*, 2000, **97**, 11922.
53 G. Veglia, F. Porcelli, T. DeSilva, A. Prantner and S. J. Opella, *J. Am. Chem. Soc.*, 2000, **122**, 2389.
54 T. M. DeSilva, G. Veglia, F. Porcelli, A. M. Prantner and S. J. Opella, *Biopolymers*, 2002, **64**, 189.
55 L. A. Basile and J. E. Coleman, *Protein Sci.*, 1992, **1**, 617.
56 M. Koch, S. Bhattacharya, T. Kehl, M. Gimona, M. Vašák, W. Chazin, C. W. Heizmann, P. M. H. Kroneck and G. Fritz, *Biochim. Biophys. Acta*, 2007, **1773**, 457.
57 W. Lu and M. J. Stillman, *J. Am. Chem. Soc.*, 1993, **115**, 3291.
58 M. R. Ghadiri and C. Choi, *J. Am. Chem. Soc.*, 1990, **112**, 1630.
59 L. Hemmingsen, K. N. Sas and E. Danielsen, *Chem. Rev.*, 2004, **104**, 4027.
60 T. Butz, W. Tröger, T. Pöhlmann and O. Nuyken, *Z. Naturforsch.*, 1992, **47a**, 85.
61 W. Tröger, *Hyperfine Interact.*, 1999, **120/121**, 117.
62 P. Gockel, M. Gelinsky, R. Vogler and H. Vahrenkamp, *Inorg. Chim. Acta*, 1998, **272**, 115.
63 M. Rowinska-Zyrek, D. Witkowska, S. Bielinska, W. Kamysz and H. Kozlowski, *Dalton Trans.*, 2011, **40**, 5604.

64 H. Reyes-Caballero, G. C. Campanello and D. P. Giedroc, *Biophys. Chem.*, 2011, **156**, 103.
65 M. A. Pennella, A. I. Arunkumar and D. P. Giedroc, *J. Mol. Biol.*, 2006, **356**, 1124.
66 C. Migliorinia, E. Porciatti, M. Luczkowski and D. Valensina, *Coord. Chem. Rev.*, 2012, **256**, 352.
67 K. Kulon, D. Woźniak, K. Wegner, Z. Grzonka and H. Kozłowski, *J. Inorg. Biochem.*, 2007, **101**, 1699.
68 C. Kállay, K. Ősz, A. Dávid, Z. Valastyán, G. Malandrinos, N. Hadjiliadis and I. Sóvágó, *Dalton Trans.*, 2007, 4040.
69 C. Kállay, K. Várnagy, G. Malandrinos, N. Hadjiliadis, D. Sanna and I. Sóvágó, *Inorg. Chim. Acta*, 2009, **362**, 935.
70 P. Andersson, J. Kvassman, A. Lindström, B. Oldén and G. Pettersson, *Eur. J. Biochem.*, 1980, **108**, 303.
71 L. Hemmingsen, R. Bauer, M. J. Bjerrum, M. Zeppezauer, H. W. Adolph, G. Formicka and E. Cedergren-Zeppezauer, *Biochemistry*, 1995, **34**, 7145.
72 K. L. Bren, Nuclear Magnetic Resonance (NMR) Spectroscopy of Metallobiomolecules, in *Encyclopedia of Inorganic and Bioinorganic Chemistry*, John Wiley & Sons, Ltd., 2011, DOI: 10.1002/9781119951438.eibc0296.
73 M. Ringkjøbing Jensen, M. A. S. Hass, D. F. Hansen and J. J. Led, *Cell. Mol. Life Sci.*, 2007, **64**, 1085.
74 P. Atkins and J. de Paula, Reaction dynamics, in *Physical Chemistry*, W. H. Freeman and Company, New York, 9th edn, 2010, ch. 22, pp. 831–875.
75 R. A. Pufahl, C. P. Singer, K. L. Peariso, S.-J. Lin, P. J. Schmidt, C. J. Fahrni, V. Cizewski Culotta, J. E. Penner-Hahn and T. V. O'Halloran, *Science*, 1997, **278**, 853.
76 A. K. Boal and A. C. Rosenzweig, *Chem. Rev.*, 2009, **109**, 4760.
77 D. T. Richens, *The Chemistry of Aqua Ions: Synthesis, Structure and Reactivity: A Tour Through the Periodic Table of the Elements*, John Wiley & Sons, Chichester, 1997.
78 R. Pribil, *Applied Complexometry*, ed. R.A. Chalmers, Pergamon Press, Oxford, UK, 1982.
79 A. J. Miles, R. W. Janes, A. Brown, D. T. Clarke, J. C. Sutherland, Y. Tao, B. A. Wallace and S. V. Hoffmann, *J. Synchrotron Radiat.*, 2008, **15**, 420.
80 A. J. Miles, S. V. Hoffmann, Y. Tao, R. W. Janes and B. A. Wallace, *Spectroscopy*, 2007, **21**, 245.
81 O. Iranzo, P. W. Thulstrup, S. B. Ryu, L. Hemmingsen and V. L. Pecoraro, *Chem. – Eur. J.*, 2007, **13**, 9178.
82 R. J. Beynon and J. S. Easterby, *Buffer Solutions*, Taylor & Francis, UK, 2003.
83 *ACD/Spectrus Processor, version 2012 (Build 61851, 24 Jan 2013)*, Advanced Chemistry Development, Inc., Toronto, ON, Canada, http://www.acdlabs.com, 2012.
84 L. Zékány, I. Nagypál and G. Peintler, *PSEQUAD for Chemical Equilibria*, Technical Software Distributors, Baltimore, MD, 1991.